First-Principles Ion−Water Interaction Potentials for Highly Charged Monatomic Cations. Computer Simulations of Al^{3+}, Mg^{2+}, and Be^{2+} in Water

José M. Martínez, Rafael R. Pappalardo, and Enrique Sánchez Marcos*

Contribution from the Departamento de Química Física, Universidad de Sevilla, 41012-Sevilla, Spain

Received August 26, 1998. Revised Manuscript Received January 19, 1999

Abstract: The concept of hydrated ion $[M(H_2O)_m]^{n+}$ has been used to describe interactions of highly charged monatomic cations in water. Ab initio interaction potentials for Al^{3+}, Mg^{2+}, and Be^{2+} have been developed on the basis of that previously applied to the Cr^{3+} hydration study (Martínez et al. *J. Chem. Phys.* **1998**, *109*, 1445). Transferability of the different contributions to the intermolecular potentials that describe the interactions between the central cation and the first hydration shell, $M^{n+}-(H_2O)_l$, and the hydrate with bulk water molecules, $[M(H_2O)_m]^{n+}-(H_2O)_{bulk}$, have been examined. Results indicate that a reduced number of points (∼40 quantum chemical computations) are enough to get the basic and differential features of each cation. MD simulations (200 ps) for the hydrate of each cation plus 512 TIP4P H_2O have been performed. Structural properties such as RDFs among different pairs of atoms in the system and orientational parameter are presented. Likewise, dynamical properties such as self-diffusion coefficients, reorientational and mean residence times, and power spectra have been obtained and analyzed. The comparative study of the properties derived from the hydration of each cation and the degree of transferability of the intermolecular potentials based on their main features is thoroughly discussed. Prospectives and benefits introduced by this type of flexible hydrated ion−water interaction potential in molecular simulations are pointed out.

Introduction

The study of metal ions in solution is one of the most active areas in solution chemistry due to the large number of physicochemical and biochemical properties directly controlled or indirectly conditioned by ionic effects in many fields of chemistry, biochemistry, and chemical engineering.[1−5]

Due to the large number of particles forming these systems and to the variety of different interactions established, computer simulations represent a particularly adequate theoretical tool for understanding and predicting at the microscopical level the physicochemical properties of these solutions.[6−8] Intermolecular potentials are a key point of these computations, and their determination appears, consequently, as one of the most important activities in the field.[9] The possibility of obtaining these potentials from quantum-chemical calculations allows first-principles-based statistical simulations which usually facilitates the design of improving strategies.[6] Against this fundamental advantage, the computational cost and the many-body terms that are associated with the ion−solvent interactions made difficult, and sometimes unpractical, their determination when compared to empirically fitted potentials.[9,10] A representative example of this situation is that of salt effects on conformational changes and binding reactions involving nucleic acids and other important biomolecules.[11−16] Several sophisticated general force fields have been developed and largely tested in the literature, allowing successful modeling of complex biomolecular problems.[17,18] However, effects due to the largely microscopic heterogeneity of hydrated counterions are, in general, poorly described, and some empirical corrections are usually introduced to modulate their role in these solutions.[13,19] The more highly charged counterions are, the more complicated the situation becomes.

An old electrochemical concept recognizes that some ions, mainly metal and highly charged monatomic cations (M^{n+}), in

* Corresponding author: (e-mail) sanchez@mozart.us.es.

(1) Burgess, J. *Metal Ions in Solution*; Ellis Horwood: New York, 1978.
(2) Conway, B. E. *Ionic Hydration in Chemistry and Biophysics. Studies in Physical and Theoretical Chemistry*; Elsevier: Amsterdam, 1981; Vol. 12.
(3) Marcus, Y. *Ion Solvation*; Wiley: Chichester, 1986.
(4) Barthel, J. M. G.; Krienke, H.; Kunz, W. *Physical Chemistry of Electrolyte Solutions*; Steinkopff: Darmstadt, 1998.
(5) Warshel, A. *Computer Modeling of Chemical Reactions in Enzymes and Solutions*; John Wiley: New York, 1991.
(6) Clementi, E. In *Modern Techniques in Computational Chemistry*; Escom: Leiden, 1990; Chapter I.
(7) Allen, M. P.; Tildesley, D. J. *Computer Simulation of Liquids*; Oxford University Press: Oxford, 1987.
(8) Simkin, B. Y.; Sheikhet, I. I. *Quantum Chemical and Statistical Theory of Solutions: A Computational Approach*; Ellis Horwood: London, 1995.
(9) Stone, A. J. *The Theory of Intermolecular Forces*; Clarendon Press: Oxford, 1996.
(10) Elrod, N. J.; Saykally, R. J. *Chem. Rev.* **1994**, *94*, 1975.
(11) Haseth, P. L.; Lohman, T. M.; Record, M. T. *Biochemistry* **1977**, *16*, 4783.
(12) Honig, B.; Nicholls, A. *Science* **1995**, *268*, 1144.
(13) Montoro, J. C. G.; Abascal, J. L. F. *J. Chem. Phys.* **1995**, *103*, 8273.
(14) Perkyns, J. S.; Wang, Y.; Pettitt, B. M. *J. Am. Chem. Soc.* **1996**, *118*, 1164.
(15) Young, M. A.; Jayaram, B.; Beveridge, D. L. *J. Am. Chem. Soc.* **1997**, *119*, 59.
(16) Jayaram, B.; Beveridge, D. L. *Annu. Rev. Biophys. Biomol. Struct.* **1996**, *25*, 367.
(17) Dinur, U.; Hagler, A. T. In *Reviews in Computational Chemistry*; Lipkowitz, K. B., Boyd, D. B., Eds.; VCH: Leiden, 1991; Vol. 2, Chapter 4.
(18) Pettersson, I.; Liljefors, T. In *Reviews in Computational Chemistry*; Lipkowitz, K. B., Boyd, D. B., Eds.; VCH: New York, 1996; Vol. 9, Chapter 4.
(19) Singh, U. C.; Weiner, S. J.; Kollman, P. *Proc. Natl. Acad. Sci. U.S.A.* **1985**, *82*, 755.

10.1021/ja9830748 CCC: $18.00
Published on Web 03/23/1999

aqueous and other polar solvent solutions (S), behave as more complex entities than expected.[20] The representative aggregate in solution, $[M(S)_m]^{n+}$, was called solvated ion (hydrated ion when $S = H_2O$). This idea has been employed in computer simulations of proteins in solution to justify the large ionic effective radii for monatomic cations which accounted for the effect of aqueous hydration.[19]

Our group used this concept within statistical simulations by considering that the ion interacts in aqueous solution via its hydrated form.[21] Thus, ab initio $[M(H_2O)_6]^{n+}-H_2O$ intermolecular potentials were developed for Zn^{2+} and Cr^{3+}. This was called the hydrated ion−water potential (HIW) and tested by Monte Carlo (MC)[21−23] and molecular dynamics (MD)[24] simulations. Hydration of these difficult cations has been satisfactorily described, as energetic, structural, and dynamical properties were simultaneously fairly reproduced without inclusion of any correcting terms in the proposed potentials. More recently,[25] the rigidity of the hydrate has been released by adding to the original HIW potential a complementary potential. This new potential, the ion−water first shell (IW1), accounts for the inner dynamics of the first-shell water molecules and the Cr^{3+} cation. Nevertheless, there is a double limitation in the method to obtain the HIW and IW1 potentials. The first one is the large number of quantum chemical single points (∼1200) that are needed to properly sample the potential energy surface that comes from the interaction between the hydrate and a probe water molecule. A second limitation is the finding of a reliable fit for a given functional form that reproduces as close as possible the ab initio interaction energies. A priori this fact is never guaranteed. Dissemination of such a type of effective ab initio potentials depends on the finding of a low-cost technique to build reliable potentials for other cations. In this sense, the finding of *transferable* contributions in the HIW and IW1 potentials among cations retaining their peculiar features is of great interest. This is the main goal of this work: to check if the already developed potential for Cr^{3+} ion can be easily reused, for a given set of cations saving as much as possible additional computational and analytical efforts.

Cations on which new hydrated ion potentials are developed were chosen on the basis of three criteria. The first requirement is imposed by the physicochemical basis of the method: mean residence time of water molecules in the first shell should be at least 1 order of magnitude larger than the total simulation time.[3] The second one is a methodological point: changes in cation properties must be progressive to test the degree of transferability of the hydrated ion model. Finally, the third one is chemical:the choice of cations that satisfy the previous conditions were of high chemical interest.[20] The following cations, among others, fulfill those conditions: Al^{3+}, Mg^{2+}, and Be^{2+}.[26−28] The first one is close to the starting point, that is the potential for the Cr^{3+} hexahydrate, although the chemical nature of Cr−O bonding has a much larger covalent character than that of Al−O.[20,28] The second cation, Mg^{2+}, retains a coordination number of six in the first shell, but charge is decreased with respect to the chromium case. Finally, Be^{2+} changes its hydration sphere with respect to the previous ones, adopting a tetrahedral coordination.[20] For the divalent cations, several authors have performed simulations in order to get a microscopic description of the hydration of these small ions.[29−37] These are representative systems where the pairwise additivity in the interactions is lost.[10] On the contrary, and to our best knowledge, there is only one MD simulation of Al^{3+} in water, based on an ab initio hexahydrate−water interaction potential.[38] Apart from methodological reasons, Al^{3+} and Be^{2+} are recognized to be active toxicological agents in solution,[38−40] whereas Mg^{2+} is one of the most important oligoelements present in a living being.[41,42] Several groups have also proposed in several ways, applications of the hydrated ion concept, to build intermolecular potentials of metal cations. Their results also point out the advantages of this approach in describing equilibrium physicochemical properties of ionic solutions.[35,36,38,43−45] All of these applications can be classified within the framework of effective potentials in classical statistical models. There is a rather different perspective which is connected to the use of an instantaneous quantum chemical description of the hydration by means of ab initio MD simulations[46] (AIMD) or hybrid methods such as quantum mechanics/molecular mechanics techniques[47−49] which combine the advantages of a precise description of the solute's environment with statistical information derived from classical statistical techniques. However, a crucial limitation of these strategies is the computational cost that limits, in particular the more rigorous AIMD, the system size and simulation time. Marx et al.[37] have recently applied the Carr−Parrinello method to describe Be^{2+} hydration. Due to the high computational cost of this technique, the system was formed by a Be^{2+} cation and 32 H_2O, and 1 ps was the

(20) Richens, D. T. *The Chemistry of Aqua Ions*; John Wiley: Chichester, 1997.
(21) Pappalardo, R. R.; Sanchez Marcos, E. *J. Phys. Chem.* **1993**, *97*, 4500.
(22) Pappalardo, R. R.; Martinez, J. M.; Sanchez Marcos, E. *J. Phys. Chem.* **1996**, *100*, 11748.
(23) Sánchez Marcos, E.; Martinez, J. M.; Pappalardo, R. R. *J. Chem. Phys.* **1996**, *105*, 5968.
(24) Martínez, J. M.; Pappalardo, R. R.; Sánchez Marcos, E.; Refson, K.; Díaz-Moreno, S.; Muñoz-Páez, A. *J. Phys. Chem. B* **1998**, *102*, 3272.
(25) Martínez, J. M.; Pappalardo, R. R.; Sánchez Marcos, E. *J. Chem. Phys.* **1998**, *109*, 1445.
(26) Bock, C. W.; Glusker, J. P. *Inorg. Chem.* **1993**, *32*, 1242.
(27) Bock, C. W.; Kaufman, A.; Glusker, J. P. *Inorg. Chem.* **1994**, *33*, 419.
(28) Akesson, R.; Pettersson, G. M.; Sandstrom, M.; Wahlgren, U. *J. Am. Chem. Soc.* **1994**, *116*, 8691.
(29) Yamaguchi, T.; Ohtaki, H.; Spohr, E.; Palinkas, G.; Heinzinger, K.; Probst, M. M. *Z. Naturforsch.* **1986**, *41A*, 1175.
(30) Probst, M. M.; Spohr, E.; Heinzinger, K. *Chem. Phys. Lett.* **1989**, *161*, 405.
(31) Probst, M. M. *Chem. Phys. Lett.* **1987**, *137*, 229.
(32) Probst, M. M.; Spohr, E.; Heinzinger, K.; Bopp, P. *Mol. Simul.* **1991**, *7*, 43.
(33) Aqvist, J. *J. Phys. Chem.* **1990**, *94*, 8021.
(34) Bernal-Uruchurtu, M. I.; Ortega-Blake, I. *J. Chem. Phys.* **1995**, *103*, 1588.
(35) Periole, X.; Allouche, D.; Daudey, J. P.; Sanejouand, Y. H. *J. Phys. Chem. B* **1997**, *101*, 5018.
(36) Periole, X.; Allouche, D.; Ramirez-Solis, A.; Ortega-Blake, I.; Daudey, J. P.; Sanejouand, Y. H. *J. Phys. Chem. B* **1998**, *102*, 8579.
(37) Marx, D.; Sprik, M.; Parrinello, M. *Chem. Phys. Lett.* **1997**, *273*, 360.
(38) Wasserman, E.; Rustad, J. R.; Xantheas, S. *J. Chem. Phys.* **1997**, *106*, 9769.
(39) Parker, D. R.; Kinraide, T. B.; Zelazny, L. W. *Soil. Sci. Soc. Am. J.* **1989**, *53*, 789.
(40) Skilleter, D. N. *Chem. Ber.* **1990**, *26*, 26.
(41) Tainer, J. A.; Roberts, V. A.; Getzoff, E. D. *Curr. Opin. Biotechnol.* **1991**, *2*, 582.
(42) Christianson, D. W. *Adv. Protein Chem.* **1991**, *42*, 281.
(43) Bleuzen, A.; Foglia, F.; Huret, E.; Helm, L.; Merbach, A. E.; Weber, J. *J. Am. Chem. Soc.* **1996**, *118*, 12777.
(44) Floris, F.; Persico, M.; Tani, A.; Tomasi, J. *Chem. Phys. Lett.* **1992**, *199*, 518.
(45) Cordeiro, M. N. D. S.; Gomes, J. A. N. F. *J. Comput. Chem.* **1993**, *14*, 629.
(46) Carr, R.; Parrinello, M. *Phys. Rev. Lett.* **1985**, *55*, 2471.
(47) Gao, J. In *Reviews in Computational Chemistry*; Lipkowitz, K. B., Boyd, D. B., Eds.; VCH: New York, 1996; Vol. 7, Chapter 3.
(48) Warshel, A. *J. Phys. Chem.* **1979**, *83*, 1640.
(49) Field, M. J.; Basch, P. A.; Karplus, M. *J. Am. Chem. Soc.* **1987**, *109*, 8092.

total simulation time. An example of the hybrid methodology is the DFT/MC study of bromide hydration by Tuñón et al.[50]

In this sense, the type of potentials we propose may contribute to satisfy the actual requirement for describing ion interactions in solution accurately enough, but maintaining the computational cost low enough to carry out representative simulations.

Methodology

Outline of the Hydrated Ion Model. The key point for such a model is to consider the water molecules closer to the ion as forming part of the solute and not of the solvent bulk. These molecules are so highly perturbed by the ion that they must no longer be considered solvent molecules, but rather forming part of the solute in a supermolecule entity called the hydrated ion (HI). Keeping that in mind, if one wants to perform an statistical simulation to study the hydration of a given ion, two steps must be completed. In the first one, the hydrated ion may be envisaged like a *rigid* unit which evolves through the solution without changing its internal geometry. This approach needs the development of an interaction potential between such a unit and the solvent molecules, i.e., the HIW potential. The details about the building of the $[M(H_2O)_m]^{n+}-H_2O$ intermolecular potential can be found in references 21 and 22. The HIW expression, built on the basis of site−site distances r_{ij}, contains two contributions: one of them accounts for long-range interactions, and the other for short-range interactions that are described by a linear combination of r^{-n} ($n > 3$) terms:

$$E_{\mathrm{HIW}} = \sum_{i}^{\text{HI sites}} \sum_{j}^{\text{W sites}} \frac{C_4^{ij}}{r_{ij}^4} + \frac{C_6^{ij}}{r_{ij}^6} + \frac{C_{12}^{ij}}{r_{ij}^{12}} + \frac{q_i q_j}{r_{ij}} \qquad (1)$$

To obtain reliable potentials, a large number (>1200 points) of quantum mechanical structures of the hydrate and the probe water molecule have to be computed. This approach allows us to extract statistical information of the aqua ion when the simulation is performed and, in the case of the solvent, properties beyond the first hydration shell. The lack of information regarding the dynamics of the first solvation sphere as well as the rigidity effects of the aggregate on the rest of the solution has been criticized by some authors.[34,43,51] To avoid it, one can afford the second step, *a flexible hydrated ion model*. In this case, the use of interaction potentials among the components of the hydrate is mandatory, which should describe properly the dynamics of their interactions. At the same time, it is desirable to keep the accuracy reached in the solvation description of the aquaion by means of the HIW potential. The strategy we propose, previously applied to the $[Cr(H_2O)_6]^{3+}$ case,[25] is based on the development of an effective bare ion−water pair interaction potential, built from first principles. It has to take into account the important many-body effects present in the nearest neighborhood of the cation. This new potential, IW1, will not impose any translational or rotational constraints to the water molecules of the first shell (Figure 1). The functional form that describes the interactions $M^{n+}-H_2O$ is similar to that used for the HIW potential: a Coulombic part plus a linear combination of r^{-n} terms which represent the short-range contribution. It is worth pointing out that water−water interactions are present as well in the description of the aqua ion and are taken into account in the extraction process of IW1. Details about the building of IW1 can be found in reference 25. Its construction for the case of the cations here considered will be outlined below. The interactions between the hydrated (and now flexible) ion and the solvent molecules will be described by the original HIW interaction potential. Figure 1 shows the solution model defined and the physical regions around the cation in which the HIW and IW1 potentials are applied. Within the inner region, water molecules of the first shell, which are strongly polarized and with a partial charge transferred, interact with the cation by means of the IW1 and among them by a standard water model (in our case TIP4P[52]) but where the charges and geometry are those derived from the quantum chemical computations of the hydrate. In the outer region, the water molecule interacts with the hydrate by the HIW potential and among them by the chosen standard water model (TIP4P). It may be thought whether the influence of the hydrated ion on the structure of second-shell water molecules may force the use of a flexible water model. However, quantum chemical computations for large water clusters of several divalent cations have shown that the changes of the OH bonds and HOH angles for molecules in the second shell are less than 2 mÅ and below 1°, respectively.[53,54]

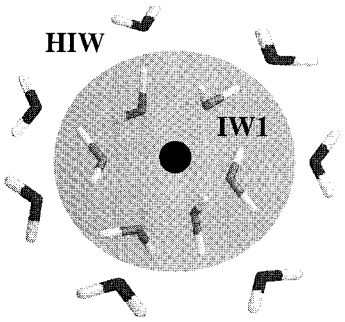

Figure 1. Schematic representation of the regions where the two ion−water interaction potentials are defined: IW1, ion−water of the first shell, and HIW, hydrated ion−water of the bulk.

Quantum Chemical Computations. Once the hydration number for a given cation is known,[1−3,20,55,56] the reference structure for its hydrate is obtained by an optimization of the corresponding cluster $[M(H_2O)_m]^{n+}$ under the density functional theory formalism using the hybrid exchange correlation Becke 3-Lee−Yang−Parr functional (B3LYP).[57] Correlation consistent polarized valence basis sets[58,59] of triple-ζ quality, cc-pVTZ, were used for the metal ions, while water molecules were described by basis sets of double-ζ quality increased with diffuse functions, aug-cc-pVDZ.[59,60] Calculations were carried

(50) Tuñon, I.; Martins-Costa, M. T. C.; Millot, C.; Ruíz-López, M. F. *Chem. Phys. Lett.* **1995**, *241*, 450.

(51) Bernal-Uruchurtu, M. I.; Hernandez-Cobos, J.; Ortega-Blake, I. *J. Chem. Phys.* **1998**, *108*, 1750.

(52) Jorgensen, W. L.; Chandrasekhar, J.; Madura, J. D.; Impey, R. W.; Klein, M. L. *J. Chem. Phys.* **1983**, *79*, 926.

(53) Pavlov, M.; Siegbahn, P. E. M.; Sandstrom, M. *J. Phys. Chem. A* **1998**, *102*, 219.

(54) Markham, G. D.; Glusker, J. P.; Bock, C. L.; Trachtman, M.; Bock, C. W. *J. Phys. Chem.* **1996**, *100*, 3488.

(55) Ohtaki, H.; Radnai, T. *Chem. Rev.* **1993**, *93*, 1157.

(56) Magini, M.; Licheri, G.; Paschina, G.; Piccaluga, G.; Pinna, G. *X-Ray Diffraction of Ions in Aqueous Solutions*: *Hydration and Complex Formation*; CRC Press: Boca Raton, FL, 1988.

(57) Becke, A. D. *J. Chem. Phys.* **1993**, *98*, 5648.

(58) Woon, D.; Dunning, T. H. J. *J. Chem. Phys.* **1993**, *98*, 1358.

(59) Feller, D. Basis sets were obtained from the Extensible Computational Chemistry Environment Basis Set Database, Version 1.0, as developed and distributed by the Molecular Science Computing Facility, Environmental and Molecular Sciences Laboratory, which is part of the Pacific Northwest Laboratory, P.O. Box 999, Richland, WA 99352, and funded by the U.S. Department of Energy. The Pacific Northwest Laboratory is a multiprogram laboratory operated by Battelle Memorial Institute for the U.S. Department of Energy under Contract DE-AC06-76RLO 1830. Contact David Feller, Karen Schuchardt, or Don Jones for further information.

(60) Dunning, T. H. J. *J. Chem. Phys.* **1989**, *90*, 1007.

Table 1. Optimized Geometry and Binding Energy, ΔE, at the B3LYP Level[a]

hydrate	symmetry	R(M−O)	R(O−H)	∠HOH	ΔE
$[A1(H_2O)_6)]^{3+}$	T_h	1.934 (1.911)	0.977 (0.972)	107.0 (106.6)	−703.3 (−723.7)
$[Mg(H_2O)_6)]^{2+}$	T_h	2.094 (2.08)	0.968 (0.978)	106.2 (110.3)	−320.3 (−303.9)
$[Be(H_2O)_4)]^{2+}$	S_4	1.646 (1.65)	0.973 (0.982)	107.8 (110.7)	−397.6 (−384.4)

[a] Distances in Å, angles in deg, and energies in kcal mol $^{-1}$. [b] Values in parentheses are recent quantum chemical computations obtained by Wasserman et al.[38] for aluminum and by Pavlov et al.[53] for magnesium and beryllium.

out with Gaussian94 package.[61] Table 1 collects the main geometrical parameters for the three hydrates and their corresponding formation energies,

$$\Delta E = E_{[M(H_2O)_m]^{n+}} - mE_{H_2O} - E_{M^{n+}} \qquad (2)$$

For the sake of comparison, our results are compared in the same table with others recently obtained by other authors with larger basis sets, at different levels of computations. Stationary points on the potential energy hypersurface were characterized by harmonic frequency analysis and found to be minimums.

In our previous Cr^{3+} hydration statistical studies,[22,24,25] the hydrate was optimized inside a cavity using the self-consistent reaction field (SCRF) methodology developed by the Nancy group.[62] In this way, bulk effects (present in polar and ionic condensed media) on the hydrated ion were included. This approximation has been successfully applied to the energetics of the cation hydration.[63] However, a recent study[64] on ion solvation has shown that continuum models, when only the first hydration sphere is present inside the cavity, cause an increase in the M−O_I distance. This should be counterbalanced by the specific first−second hydration shells interactions, leading to a nearly complete cancellation of both effects. Thus, to avoid such a model-dependent tendency for the cations considered in this work, full geometry optimizations were performed in gas phase. Nonetheless, the wave function that describes the ground state of the relaxed geometry was polarized by the effects of the continuum, following the PCM method of Tomasi's group.[65] Both (HIW and IW1) potentials use effective atomic electrostatic charges derived from a fitting procedure to reproduce the molecular electrostatic potential generated by the solute's wave function, which is already polarized by the bulk solvent. The recommendation recently given by Sigfridsson and Ryde[66] has been followed: charges were obtained using the Merz−Kollman method[67,68] with a high point density (∼2000 points/atom).

Extending the Flexible HI Model to Al^{3+}, Mg^{2+}, and Be^{2+}. The results obtained with the flexible HI model developed for Cr^{3+} show a well-balanced combination between the internal and external potentials of the hydrate.[25] However, as mentioned in the Introduction, the extension of the model, as it is, to other cations is seriously limited by the high computational cost needed for its building.

Table 2. Summary of the Transferable or Specific Character of the Different Contributions in the Interaction Potentials[a]

potential	transferable		specific	
HIW	short range ($C_{4,6,12}$)	1200	electrostatics	1
IW1	short-range H_2O-H_2O	0	electrostatics	1
			short range M−H_2O	40

[a] Number of quantum chemical computations needed for each contribution are specified as well.

HIW and IW1 potentials, as mentioned before, can be split into two different terms: electrostatics and short range. Table 2 shows the number of quantum chemical computations needed for the definition of each term. The success in the generalization of the potentials will be based on a good choice for what can be transferable when going from Cr^{3+} to other ions and what cannot be. Regarding electrostatics, both potentials use the set of charges derived from the molecular wave function of the hydrate. Taking into account that the total charge of the hydrate depends on the ion, it is obvious that this contribution cannot be transferable. The nature of the chemical bonding between the bare ion and the first-shell water molecules is projected, in some way, in the short-range contribution of IW1, so this is again very specific for each ion. The short-range contribution to the HIW potential basically defines the van der Waals surface of the hydrate, which is more dependent on the water molecules than on the cation. Although this topological consideration is known to be very important for a proper description of the hydrate surrounding,[24,69] it may be considered as transferable among aqua ions, specially if it is implicitly modified by specific features of the hydrate that are taken into account during the potential building: M−O_I distance, first-shell water molecule geometry, number of water molecules, and shrinkage or expansion of the surface due to the electrostatic contribution. It is obvious (Table 2) that this is the most desirable part to be transferable.

Following these assumptions, the steps needed for the development of Al^{3+}, Mg^{2+}, and Be^{2+} IW1 and HIW potentials are the following: (1) optimization of the hydrate in gas phase; (2) single-point computation of the hydrate at the gas-phase optimized geometry within a dielectric continuum (SCRF calculation); (3) fitting of effective charges on the atoms using the wave function polarized by the solvent continuum model; (4) sampling of the intracluster potential energy moving one water molecule of the hydrate along the metal−oxygen axis; (5) fitting of the coefficients that describe the short-range term in IW1, once the electrostatic and water−water short-range interactions are subtracted.

For the three cases here considered, scans were performed with 40 single-point computations which covered the interval [R^{opt}_{M-O} − 0.2 Å, R^{opt}_{M-O} + 0.2 Å]. In all cases, fair fittings, standard deviations below 0.02 kcal/mol, were found using the

(61) Frisch, M. J.; Trucks, G. W.; Schlegel, H. B.; Gill, P. M. W.; Johnson, B. G.; Robb, M. A.; Cheeseman, J. R.; Keith, T.; Petersson, G. A.; Montgomery, J. A.; Raghavachari, K.; Al-Lahami, M. A.; Zakrzewski, V. G.; Ortiz, J. V.; Foresman, J. B.; Cioslowski, J.; Stefanov, B. B.; Nanayakkara, A.; Challacombe, M.; Peng, C. Y.; Ayala, P. Y.; Chen, W.; Wong, M. W.; Andres, J. L.; Replogle, E. S.; Gomperts, R.; Martin, R. L.; Fox, D. J.; Binkley, J. S.; Defrees, D. J.; Baker, J.; Stewart, J. P.; Head-Gordon, M.; Gonzalez, C.; Pople, J. A. *Gaussian 94, Revision E.2.*; Gaussian Inc.: Pittsburgh PA, 1995.

(62) Rinaldi, D.; Rivail, J. L.; Rguini, N. *J. Comput. Chem.* **1992**, *13*, 675.

(63) Sánchez Marcos, E.; Pappalardo, R. R.; Rinaldi, D. *J. Phys. Chem.* **1991**, *95*, 8928.

(64) Martínez, J. M.; Pappalardo, R. R.; Sanchez Marcos, E. *J. Phys. Chem. A* **1997**, *101*, 4444.

(65) Miertus, S.; Scrocco, E.; Tomasi, J. *Chem. Phys.* **1981**, *55*, 117.

(66) Sigfridsson, E.; Ryde, U. *J. Comput. Chem.* **1998**, *19*, 377.

(67) Sing, U. C.; Kollman, P. A. *J. Comput. Chem.* **1984**, *5*, 129.

(68) Besler, B. H.; Merz, K. M.; Kollman, P. A. *J. Comput. Chem.* **1990**, *11*, 431.

(69) Martínez, J. M.; Pappalardo, R. R.; Sánchez Marcos, E. *J. Chem. Phys.* **1999**, *110*, 1669.

Table 3. Fitted Parameters of the HIW and IW1 Potentials (Eqs 1 and 3)

cation	q_M	q_O	q_H	*A*	*B*	*C*	*D*
Al^{3+}	2.3250	−1.0621	0.5873	−7581.68	67055.75	−82910.56	66666.02
Mg^{2+}	2.2724	−1.1242	0.5394	3047.22	−29951.16	43033.97	−49135.97
Be^{2+}	1.7208	−1.1344	0.6021	−1932.29	12687.27	−13094.02	4226.25

following expression for IW1:

$$E_{IW1} = \frac{A}{r_{MO}^4} + \frac{B}{r_{MO}^6} + \frac{C}{r_{MO}^7} + \frac{D}{r_{MO}^{12}} + \sum_{i}^{W\ sites} \frac{q_M q_i}{r_{Mi}} \qquad (3)$$

Table 3 collects the parameters that define IW1 potentials developed for Al^{3+}, Mg^{2+}, and Be^{2+}. When these values are used in eq 3 with distances in angstroms, the energy is given in kilocalories per mole. The HIW potential for each cation is defined by eq 1, where the charges are those of Table 3 and the *C* coefficients are those previously used for Cr^{3+} simulations (these values can be found in Table S1 of the Supporting Information of ref 24).

MD Simulation Details. Molecular dynamics simulations were performed in the microcanonical ensemble (NVE) using periodic boundary conditions. Each ionic aqueous solution contained one of the cations, six first-shell water molecules, $(H_2O)_I$, for the cases of Al^{3+} and Mg^{2+}, and four in the simulation containing Be^{2+} and 512 TIP4P water molecules acting as solvent. The basic cell was a cubic box with 24.8 Å a side. Simulations were run with the MOLDY program,[70] which is efficiently parallelized, on the HP X-Class SPP 2000 computer at CICA (Centro Informático y Científico de Andalucía). A modified form of the Beeman algorithm was used as integrator.[71] Orientations of solvent molecules, which were assumed to be rigid, were described by the quaternion formalism.[72] The time step was set up to 0.25 fs. The thermalization time was ∼40 ps, and the temperature during the following 200 ps (production period) was 298 ± 6 K. Trajectories and velocities were saved every 40 time steps.

Coulombic interactions were computed by the Edwald sum technique,[7] including the charged system term.[73] Several authors have shown the importance of its use to obtain reliable energetic, structural, and, particularly, dynamical results in the case of ionic aqueous solutions.[74−75] More details of simulation protocol can be found in previous works.[24,25]

Results and Discussion

Structural Properties. Figure 2 shows the M−O (a) and M−H (b) RDFs for solutions of the different cations. Given that simulations contain two different types of water molecules (first shell and bulk), the represented functions are the results of overimposing two RDFs for each pair. Nevertheless, these two functions describe two different regions around cations, so that the final distribution can be formally considered as the usual function. Table 4 collects the values corresponding to the maximums of the RDFs, the hydration number for the second hydration shell, and tilt angles (the angle formed by the ion−oxygen vector and the water dipole moment) of the first- and second-shell water molecules. Given the volume of information available on these ionic aqueous solutions, to simplify the comparison of the obtained results with experimental or previous theoretical data, in the same table a summary of this information has been included in parentheses. It should be pointed out that agreement with precedent available information is extremely satisfactory. This represents a support of the validity of the new developed potentials and, as a consequence, a first test of the good transferability of the potentials. The largest discrepancy is found for $R_{O_I-O_{II}}$ in the case of Mg^{2+} where an underestimation of 0.1−0.15 Å is observed. However, given the average half-width of the peaks and the approaches assumed in simulations and in models used to analyze experimental data,[20,55,56] the comparison has at least an uncertainty of ±0.05 Å. Magini et al.[56] in their excellent review on XRD study of ions in aqueous solutions stress the difficulties in obtaining oxygen−oxygen distances between hydration shells as accurately as for other pairs. M−O and M−H RDFs show that the peak width corresponding to the first shell follows the trend, $Mg^{2+} > Be^{2+} > Al^{3+}$, reflecting the different degree in which first-shell water molecules are bound to the cation. As expected, the trivalent Al^{3+} defines the narrowest region, whereas the largest divalent Mg^{2+} shows the widest one. A general trend is that M−H peaks are wider than the corresponding M−O ones, even for those peaks corresponding to the first shell. It is as a consequence of the librational and rotational movements of water molecules which affect much more the instantaneous position of hydrogens

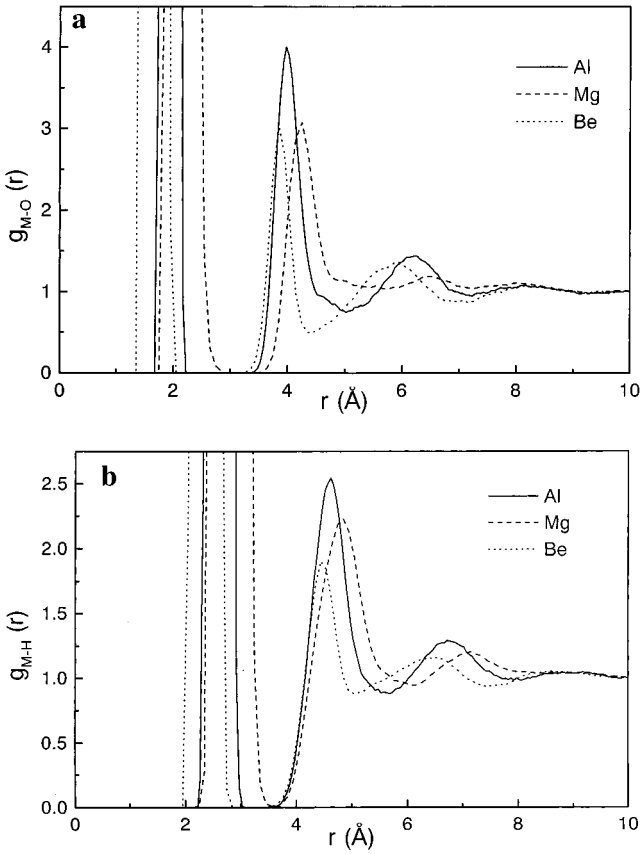

Figure 2. M−O (a) and M−H (b) RDFs for the three simulations.

(70) Refson, K. MOLDY User's Manual Rev. 2.11, Moldy code can be obtained from the CCP5 program library or by anonymous ftp from ftp.earth.ox.ac.uk.

(71) Refson, K. *Physica B&C* **1985**, *131*, 256.

(72) Goldstein, H. Classical Mechanics, 2nd ed.; Addison-Wesley: Reading, MA, 1980.

(73) Roberts, J. E.; Schnitker, J. *J. Phys. Chem.* **1995**, *99*, 1322.

(74) Perera, L.; Essmann, U.; Berkowitz, M. L. *J. Chem. Phys.* **1995**, *102*, 450.

(75) Hummer, G.; Pratt, L. R.; Garcia, A. E. *J. Phys. Chem.* **1996**, *100*, 1206.

Table 4. Structural Results. Distances (R, Å) for Ion−Oxygen and Ion−Hydrogen Maximums Corresponding to the First and Second Hydration Shells, Second Shell Hydration Number (N_{II}), Distance for Maximum of $Oxygen_I-Oxygen_{II}$ ($R_{O_I-O_{II}}$), and Tilt Angles (deg) of Water Molecules in the First (θ_I) and the Second Shells (θ_{II})

cation	R_{M-O_I}	R_{M-H_I}	$R_{M-O_{II}}$	$R_{M-H_{II}}$	N_{II}	$R_{O_I-O_{II}}$	θ_I	θ_I
Al^{3+}	1.91 (1.88−1.90)[a]	2.60(2.47)[b]	4.00 (3.98−4.04)[a]	4.62 (4.51)[b]	14 (12−14)[a]	2.57 (2.6)[c]	11(28)[b]	36
Mg^{2+}	2.08 (2.00−2.15)[d]	2.76 (2.67−2.8)[e,f]	4.25 (4.1−4.28)[d]	4.83 (4.90)[f]	13 (12)[d]	2.65 (2.75−2.81)[d]	15(14)[d]	45(53)[f]
Be^{2+}	1.65 (1.67)[g]	2.36 (2.37[h] −2.49[i])	3.87 (3.5−4.2)[h,i,j,k]	4.49 (4.36−4.55)[i]	9 (8)[l]	2.60 (2.59−2.66)[j,k]	11(20)[f]	34

[a] X-ray diffraction: (i) Bol, W.; Welzen, T. *Chem. Phys. Lett.* **1977**, 49, 189. (ii) Caminiti, R.; Licheri, G. Piccaluga, G.; Pinna, G.; Radnai, T. *J. Chem. Phys.* **1979**, *71*, 2473. (iii) Caminiti, R.; Radnai, T. *Z. Naturforsch.* **1980**, *35a*, 1368. [b] MD simulation: ref 38. [c] IR spectroscopy: ref 76 [d] X-ray and neutron diffraction: see compilation in ref 55. [e] Neutron diffraction: Skipper, N. T.; Neilson, G. W.; Cummings, S. C. *J. Phys.: Condens. Matter* **1989**, *1*, 3489. [f] MD simulations: Dietz, W.; Riede, W. O.; Heinzinger, K. *Z. Naturforsch.* **1982**, *37A*, 1038. [g] X-ray diffraction and MD simulation: ref 29. [h] MD simulation: ref 37. [i] MD simulation: ref 30. [j] Quantum mechanics computations: ref 54. [k] Quantum mechanics computations: ref 53. [l] Different experimental techniques: ref 20, p 129.

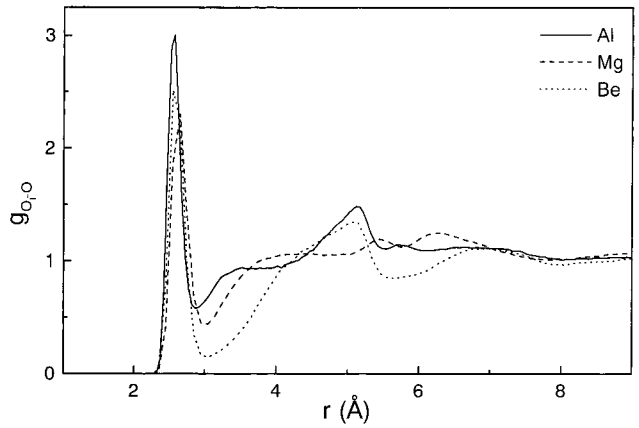

Figure 3. First-shell oxygen−bulk oxygen (O_I−O) RDF of the aqueous solutions of the three cations.

than that of oxygens. It is also noticeable that a second hydration shell is well defined in all cases. Moreover, the order around the cation extends beyond this second shell for Al^{3+} and Be^{2+}, where a quite well-defined third hydration shell is observed from M−O and M−H RDFs. Regarding tilt angle for first (θ_I) and second (θ_{II}) hydration shell water molecules, Table 4 shows how the appearance of a tilt angle for the molecules of the first shell is a direct consequence of the condensed medium, given that optimization of the hydrate in a vacuum leads in all cases to solvent molecules whose molecular plane contain the cation ($\theta_I = 0°$). As expected, the compromise among ion−water and water−water interactions leads to larger tilt angles for molecules in the second hydration shell, and the value of θ_{II} for Mg^{2+} is the largest one. The previous Cr^{3+} study[25] yielded 11 and 36°, for θ_I and θ_{II}, respectively, at the ion−oxygen distances corresponding to the RDF maximums. Average O_I-M-O_I angle determination indicates that Al^{3+} and Mg^{2+} hexahydrates adopt an octahedral disposition whereas Be^{2+} hydrate is nearly a tetrahedron with $\langle OBeO \rangle = 109.35°$.

Adopting a less Copernican perspective of the ionic solution, Figure 3 displays the O_I−O RDF for the three simulations. This function shows the distribution of water molecules around the first-shell oxygen atoms (O_I). The well-defined first peaks integrate to about two oxygen atoms, indicating two second-shell water molecules hydrogen bonded to each one of the first shell. The strong interaction between these two shells is reflected in the short $R_{O_I-O_{II}}$ (see Table 4 and first peak in RDFs of Figure 3) when compared with the typical value in pure water (a MD simulation[24] of TIP4P water liquid yields 2.80 Å and the experimental value is ∼2.85 Å). Beyond this region, the presence of a third hydration shell is observed for Al^{3+} and Be^{2+}, the corresponding maximums centered at ∼5 Å, whereas for Mg^{2+} a more diffuse structure is observed in the region 5.5−6.5. Å. Although the minimums connecting these two regions are at ∼3 Å, their depths are quite different. For the case of

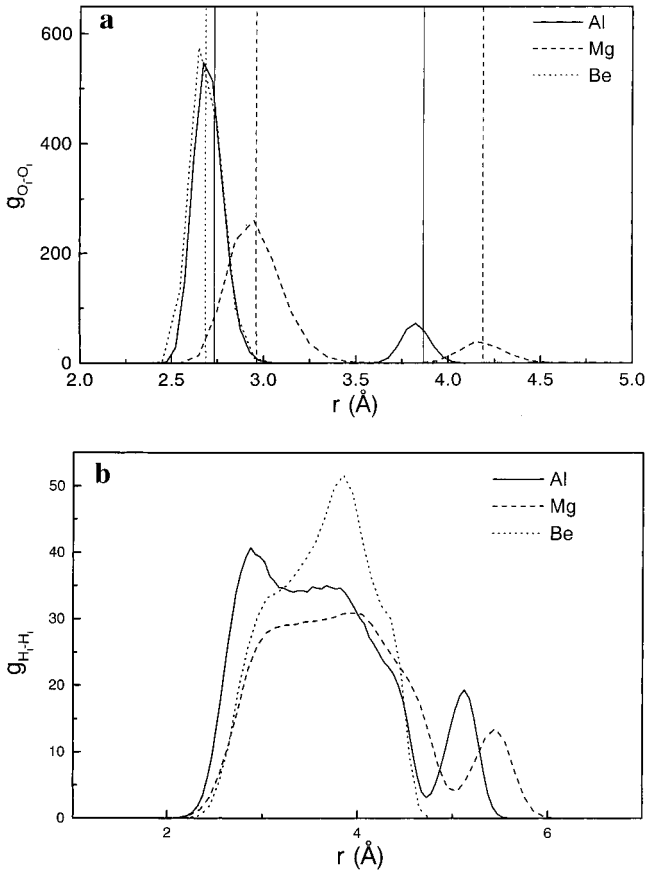

Figure 4. O_I−O_I (a) and H_I−H_I (b) RDFs. Vertical lines in (a) indicate the oxygen−oxygen distances for the quantum-mechanically optimized structure of the hydrates (see Chart 1).

Be^{2+}, it becomes almost a depletion zone, whereas the minimum value for Mg^{2+} is smaller than for Al^{3+}. This order is reflecting something more than the direct ion−water interactions, since the trivalent cation aluminum presents a lesser isolated shell than the divalent magnesium. The order observed is fairly well correlated with the density number (water molecules $Å^{-3}$) of the spherical crown of this second−third hydration shell region: 0.27 (Be^{2+}), 0.33 (Mg^{2+}), and 0.37 Å (Al^{3+}). When density increases, the water−water repulsions within the shell increase and as a consequence the rigidity and arrangement of water molecules around the acidic hydrogen atoms of the first shell are more compromised by a large number of interactions.

To get more detailed information about the structure of the first hydration shell around these cations, O_I−O_I and H_I−H_I RDFs are shown in Figure 4. To facilitate the understanding of this figure, Chart 1 displays the distances that would be found if rigid clusters of the appropriate symmetry were considered. In Figure 4a, a systematic displacement of the O_I−O_I RDF

Chart 1

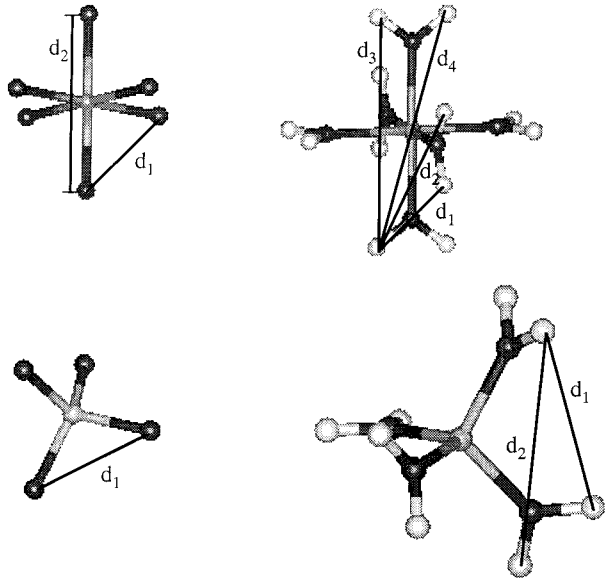

maximums with respect to the distances corresponding to the isolated $[M(H_2O)_m]^{n+}$ (vertical lines) is observed. The trend is a shortening of the O_I-O_I average distance that reflects the global effect of shrinking induced by the condensed medium on the hydrate structures. This means that specific interactions are predominant and induce a shortening of the $M-O_I$ distances.[25,53,64] O_I-O_{II} distribution shows how oxygen atoms of the first shell retain their relative positions, thus defining a tetrahedral geometry for Be^{2+} (only one peak integrating to 3) or an octahedron for Al^{3+} and Mg^{2+} (two peaks integrating to 4 and 1). The different flexibility of this first shell of oxygens is apparent by the width of the peaks. RDFs for the hydrogen atoms (Figure 4b) show in general an important loss of structure with respect to the oxygen cases. It is easily understood as a consequence of the rotational and librational movements of water molecules and indicates that these movements mainly change the relative positions of hydrogen atoms. According to Chart 1, the possible distances may be grouped into two sets for the hexahydrate pattern, a short distance including d_1 and d_2, and a long distance for d_3 and d_4. In the case of Al^{3+}, a wide peak retaining a bit of structure corresponds to the original set of "short" distances. Results previously obtained for the case of chromium solutions[25] are quite similar to those found for aluminum aqueous solutions. In the case of the Be^{2+} ion, one peak collects the two possible distances derived from the tetrahedral rigid pattern (d_1 and d_2). However, the shape of the $g_{H_I-H_I}$ function shows, as in the Al^{3+} case, that a relative order is retained. For Mg^{2+}, this wide peak has completely lost its structure, which may be attributed again to the higher degree of flexibility for the first shell of this cation. Bergstrom et al.[76] have found, by means of double-difference infrared absorption spectroscopy, evidence of a second hydration sphere in aqueous solutions of Al^{3+}, Cr^{3+}, and Rh^{3+}. The structural data here obtained for aluminum cation and those of chromium presented in a previous work,[25] at a similar level of theory and calculation, confirm the conclusions reached by these authors, which state that first−second shell interactions and structural properties among these two cations are quite similar, even though the primary $M-O_I$ distance is smaller in the aluminum case by more than 0.1 Å.

(76) Bergstrom, P.-A.; Lindgren, J.; Read, M.; Sandstrom, M. *J. Phys. Chem.* **1991**, *95*, 7650.

Dynamical Properties. To test the degree of transferability of the flexible hydrated ion−water potential and to complement the previous structural information, a set of dynamical properties has also been analyzed. Table 5 collects the values for some of these properties. Although there is some dispersion in the experimental translational self-diffusion coefficients,[55] the first conclusion is that our estimate of D values for cations (experimental estimates, in 10^{-5} cm^2 s^{-1}, are 0.53−0.72[77] for Al^{3+} and 0.70−1.1[78,79] for Mg^{2+}) on the basis of the mobility of the hydrate in aqueous solution is fairly good. This result represents an additional support to the transferability of the potentials and then to the generalization procedure. Likewise, such a fair agreement reinforces the hypothesis of the benefits that the inclusion of $[M(H_2O)_m]^{n+}$ species has in describing dynamical properties of highly charged monatomic cations in aqueous solution. Although the present model of the hydrated ion allows the independent motion of first-shell water molecules around metal ion, these molecules stay within this first shell during the whole simulation time and move with the cation through the solution. Therefore, the relative success of our strategy may also be cited as microscopic support of the role played by the hydrated ion in determining cation mobility in solution.

An interesting point is the analysis of the relative order of mobilities for this set of cations. Due to the adopted procedure, interaction potentials basically differ in specific properties of cations, and simulations have been identically performed for each cation, so that differences among ionic properties must be interpreted as having their origin in the nature of each cation and not in method-dependent artifacts. Table 5 shows that the trivalent and hexacoordinated chromium and aluminum are those having the smallest mobility. Magnesium hydrate moves slower than beryllium, what may be interpreted as meaning that the larger size of the magnesium hydrate is more important in determining D than the hydrate−water interaction energy.[80] This is consistent with a previous study[69] which showed that the increase of the ion size is not compensated by the decrease of the hydrated ion−water interaction energy, resulting in a larger mobility for the smaller ion.

Once the hydrate has been proved to be a well-defined entity in aqueous solutions for these small and highly charged cations, the rotational properties of the hydrate become an additional interesting feature of the dynamics of the solution. They are related to correlation functions,

$$C_l^i(t) = \langle P_l(\vec{u}_i(0)\cdot\vec{u}_i(t))\rangle \qquad (4)$$

where P_l is the lth Legendre polynomial and $\vec{u}_i$ is a unit vector that characterizes the orientation of the molecule. $C_l(t)$ values are computed using a coordinate frame based on the molecule. Reorientational times were obtained by fitting the $C_l(t)$ functions to a single-exponential form, i.e., $C_l(t) \sim e^{-t/\tau_l}$. These functions are involved in the definition of spectroscopic magnitudes, such as IR and Raman line shapes (τ_1 reorientational times) and NMR relaxation times (τ_2 reorientational times).[78] For practical reasons, estimated reorientational times of hydrated ions and water molecules are computed by means of ^{1}H and ^{17}O NMR techniques.[55] In this sense, the experimentally determined

(77) Herdman, G. J.; Salmon, P. S. *J. Am. Chem. Soc.* **1991**, *113*, 2930.

(78) Hertz, H. G. In *Water—A Comprehensive Treatise*; Franks, F., Ed.; Plenum: New York, 1973; Vol. 3, Chapter 7.

(79) Hewish, N. A.; Enderby, J. E.; Howells, W. S. *J. Phys. C.: Solid State Phys.* **1983**, *16*, 1777.

(80) Kay, R. L. In *Water—A Comprehensive Treatise*; Franks, F., Ed.; Plenum: New York, 1973; Vol. 3, Chapter 4, p 191.

Table 5. Dynamical Results. Translational Diffusion Coefficient D (10^{-5} cm^2 s^{-1}), Reorientational Times τ_l (ps) of l-Order ($l = 1$ or 2) for the Hydrate and the First-Shell Water Molecules,[a] and Mean Residence Times τ_{MRT} (ps) for Water Molecules in the Second Hydration Shell

	ion	hydrate[c]				$(H_2O)_I$[d]						$(H_2O)_{II}$	
cation	D	τ_1^O	τ_1^H	τ_2^O	τ_2^H	τ_1^x	τ_1^y	τ_1^z	τ_2^x	τ_2^y	τ_2^z	$\tau_{MRT}^{\tau^*=0ps}$	$\tau_{MRT}^{\tau^*=2ps}$
Al^{3+}	0.6−0.7	108	81	36	27	11.6	82.4	11.5	5.5	37.3	5.5	9.6	23.4
Cr^{3+} [b]	0.62	108	81	36	27	14	58	14	12	40	11	4.6	21
Mg^{2+}	0.7−0.8	96	84	32	28	18	100	19	9	31	9	3	14
Be^{2+}	0.9−1.0	53	40	18	14	13	52	11.5	6.5	15	6	4	23

[a] Superscript denotes axis considered (see text for hydrates and Chart 2 for water molecules). [b] Values taken from ref 25. [c] Estimated errors are ∼25%. [d] Estimated errors are ∼15%.

reorientational time is that obtained through the second-order function, τ_2. A previously proposed conclusion derived from the study of chromium solutions was an alternative definition of hydrated ion in terms of rotational dynamics. This was based on the fact that the ratio τ_1/τ_2 was exactly 3 for the hydrate, which implies that the rotation of this entity follows the Debye rotational model.[81] τ values for the three new investigated cations of Table 5 show that this behavior holds up. This is verified either when the rotation is considered taken as internal frame M−O_I vectors (τ^O) or M−H_I vectors (τ^H). According to the estimated error for this magnitude, the rotation for the three hexahydrates is quite similar, whereas the beryllium tetrahydrate rotates at higher angular velocity. Two partly overlapped reasons may be invoked to explain this different behavior: the smaller size of this last hydrate and the lower number of first−second shell hydrogen bonds. Both factors should contribute to minimize the distortion of the environment during rotation.

Experimental estimates of τ_2 for Al^{3+} is in the range of 53−44 ps from Ohtaki and Radnai's review[55] and 66.7 ps from an early work of Fiat and Connick.[82] For Mg^{2+}, the estimated value found in the literature is 13 ps.[55] Calculated values for these two hexahydrates are the same within the estimated errors. A first interpretation is that intermolecular potentials (ion−water and water−water) and/or simulation time are not able to give a fair description of this magnitude. Likewise, an alternative interpretation concerns the experimental estimate of this quantity. It is based on an specific model of cluster, where the M−H_I distance is fixed. According to the quite different dynamics of first-shell water molecules for these two cations, it is also possible that the disagreement comes, partially, from inadequacies in the approaches employed in the experimental model. At this point, it seems reasonable to compare only the order of magnitude of this property. We think this is an open question to further experimental and theoretical research. The rotational properties of first-shell water molecules have also been calculated to give a quantitative measurement of the degree in which these molecules are affected by the close presence of the cation compared with a water molecule in the pure liquid. From a previous simulation of 512 TIP4P water molecules,[24] reorientational times of a water molecule are in the ranges $\tau_1 = 3.7-2.6$ ps and $\tau_2 = 2.0-1.6$ ps. Definition of the internal frame used for water molecules is depicted in Chart 2. Data from Table 5 show that the rotational motion of a molecule in this first cosphere is highly restricted, mainly for the y axis that contains the molecular dipole moment. This fact shows that the main motion of a first-shell water molecule is the rotation around its dipole axis. This behavior is found to be more defined in the hexahydrates than in the tetrahydrate. This preferred rotational movement of first-shell water molecules allows the understanding of the different shapes observed for O_I-O_I and H_I-H_I RDFs.

Chart 2

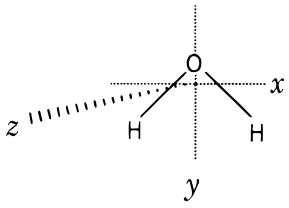

Hydrogen atoms of first-shell water molecules are the most affected by the rotation of these molecules inside this cosphere. Available experimental estimates for aluminum aqueous solution of reorientational times for water molecules have been determined by Fiat and Connick[82] to be in the range 2.34−5.75 ps.

Table 5 also includes mean residence times (MRT) for water molecules in the second hydration shell. Neither the intrinsic nature of the studied hydrates nor the model employed and simulation time allows the determination of first-shell water molecule MRT. Calculation has been carried out by the method proposed by Impey et al.[83] Within this model, t^* represents the maximum transient period that a molecule can leave the region under study without losing its ascription to this region. Values of 2 ps[83] and 0 ps[84] have been used in the literature and may be reasonably considered as values that define a significant range of MRT. Bearing in mind that these values correspond to the second hydration shell, trivalent cations present high MRT values, as well as the beryllium hydrate, in particular for $\tau_{MRT}^{t^*=2}$, whereas in the case of magnesium the values obtained are shorter. This last finding compels us to suggest that Be^{2+} is a divalent metal ion that has one of the longest lifetime for water molecules not only in the first shell,[85] but also in the second. Nonetheless, Mg^{2+} second hydration shell lifetimes still are of the same order as typical first-shell MRT of many monovalent cations.[55] This is an a posteriori support of the validity of the hydrated ion approach employed for Mg^{2+}. In addition, this finding agrees with the magnesium hydration model recently reported by Bernal−Uruchurtu and Ortega−Blake which used a polarizable water model and nonadditivity corrections for the ion−water interactions.[34]

A final test for the intermolecular potentials developed has been the determination of the power spectra for each cation and its first-shell water molecules. These spectra are obtained by applying a Fourier transform (FT) to the velocity autocorrelation function (VAC) of particles. Dynamical variables associated with the different maximums may be tentatively identified and help in the index of the intermolecular region of vibrational spectra for these electrolyte solutions.[86,87] This is a representative and sensitive test of the intermolecular potentials, since the

(81) Hansen, J. P.; McDonald, I. R. *Theory of Simple Liquids*, 2nd ed.; Academic Press: London, 1900; pp 497-508.
(82) Fiat, D.; Connick, R. E. *J. Am. Chem. Soc.* **1968**, *90*, 608.
(83) Impey, R. W.; Madden, P. A.; McDonald, I. R. *J. Phys. Chem.* **1983**, *87*, 5071.
(84) Garcia, A. E.; Stiller, L. *J. Comput. Chem.* **1993**, *14*, 1396.
(85) Cusanelli, A.; Frey, U.; Richens, D. T.; Merbach, A. E. *J. Am. Chem. Soc.* **1996**, *118*, 5265.

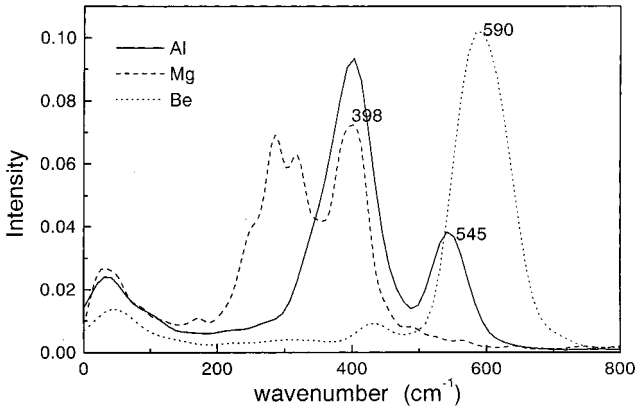

Figure 5. Power spectra for the three cations in the modeled aqueous solutions.

Table 6. Maximums Obtained from the FT of First-Shell Water Molecules VAC, $(H_2O)_I$, M−O Displacements Correlation Function δr, and O_I−M−O_I Bending Correlation Function

cation	$(H_2O)_I$	δr	bending
Al^{3+}	413, 551	413, 545	403
Mg^{2+}	307, 400	395	290
Be^{2+}	430, 594	587	430, 588

position of these bands must reflect the compromise between a refined description of the intermolecular potentials within the first hydration shell, i.e., mainly the IW1 potential, and those ones dealing with interactions between the hydrate and the rest of the solvent molecules, i.e., HIW and TIP4P potentials. Figure 5 shows the power spectra of the three cations in the modeled aqueous solution. According to the experimental values of Raman spectroscopy, the possible normal modes involving the cation, and our precedent analysis of the chromium aqueous solution simulation,[25] the peak at highest wavenumber can be assigned to the A_{1g} stretching mode for the hexahydrates (545 cm^{-1} for Al^{3+} and 398 cm^{-1} for Mg^{2+}) and to the A_1 for the Be^{2+} tetrahydrate (590 cm^{-1}). This polarized band is well reported in the literature for these cations: 532 [86]−542 [20] cm^{-1} for aluminum, 362 [86] cm^{-1} for magnesium, and 535 [86] cm^{-1} for beryllium. The agreement is fairly good in view of the low-frequency band studied. Deviations lower than 50 cm^{-1} are strong support for the general purpose intermolecular potentials here developed.

With the aim of confirming the previous index of the stretching frequency and to supply additional information on this intermolecular region of the vibrational spectra, three additional computations have been carried out. These latter results are collected in Table 6. The first column, labeled $(H_2O)_I$, shows the maximums derived from the FT of the VAC corresponding to the first-shell water molecules. In all cases, the maximum at higher wavenumber is within ±7 cm^{-1} of the same value than the peak previously assigned to the symmetric stretching mode in Figure 5. A useful way to shed light on the assignment of bands appearing in a power spectrum is the generation of correlation functions associated with dynamical variables. If they are connected with a given peak of power spectra, FT of these correlation functions must yield out values close to the previous ones. Thus, the evolution of the metal−first-shell oxygen distances can be analyzed by the correlation function

$$\langle (R_{MO_I}(0) - \overline{R_{MO_I}})(R_{MO_I}(t) - \overline{R_{MO_I}}) \rangle \qquad (5)$$

where $\overline{R_{MO_I}}$ is the mean value obtained for the whole simulation time. The average $\langle\ \rangle$ indicates not only the usual time origin average but also an average over all possible M−O pairs. The maximums obtained with this function are collected in the second column of Table 6, labeled δr, and they confirm again the index of the symmetric stretching mode presented in Figure 5, within a mean deviation of ±5 cm^{-1}. A second correlation function has been computed to tentatively index possible bending modes:

$$\langle (\cos\phi(0) - \overline{\cos\phi})\ (\cos\phi(t) - \overline{\cos\phi}) \rangle \qquad (6)$$

ϕ is the angle between two M−O bonds in the hydrate and $\overline{\cos\phi}$ is the mean value for the whole simulation. Comparison between Figure 5 and Table 6 leads to the suggestion that the peak appearing at lower frequency in the power spectra of cations may be associated with an O−M−O bending mode.

Concluding Remarks

The methodology based on the use of the flexible hydrated ion can be considered as the statistical implementation of what Henry Taube experimentally observed more than forty years ago:[88] "*The point of view which has guided the work is this: cations, perhaps all the simple ones, exert forces sufficiently strong on water molecules held in the first sphere of hydration, to make these distinguishable from other water molecules, which may also be affected. A general goal is to learn the limits for which such a distinction between 'first sphere' and remaining solvent is possible.*". This old statement emphasizes the different types of water molecules that are present in aqueous solutions containing small charged species. Monatomic and highly charged ions are paradigmatic examples of such a type of system, and the combination of the IW1 + HIW potentials to deal with their interactions in water is the proposal developed by our group to provide a first-principles-based answer. By means of the IW1 potential, a detailed quantum mechanical description of the intrinsic structural and dynamical properties of the hydrate itself is reached. It is done in such a way that many-body interactions, up to the number of particles forming the hydrate, are implicitly taken into account. The HIW potential is responsible for providing effective hydrated ion−bulk water molecule interactions. In this way, we achieve an accurate description of the interactions among the ion and the second-shell water molecules and between the first and second hydration spheres. The nuclear and electronic description of the first-shell water molecules includes polarization and charge-transfer effects, derived from the appropriate quantum chemical computation. Many-body terms are also implicitly included within the effective potential, as the probe water molecule interacts with the whole of the hydrate.

This work has established and tested a procedure to generalize the construction of the flexible hydrated ion−water potentials (IW1 + HIW) based on the analysis of the potential terms that are transferable. Transformation of the Cr^{3+} hydrate potential to those of the Al^{3+}, Mg^{2+}, or Be^{2+} hydrate only lies on the change of the charge and structure of the hydrate, which can be easily obtained by means of a reduced number of quantum-mechanical calculations. The transferability found indicates that the partition adopted by this definition of the potential is particularly appropriate to facilitate its dissemination. Its low-cost allows an easy way to generate new potentials for whatever

(86) Irish, D. E.; Brooker, M. H. In *Advances in Infrared and Raman Spectroscopies*; Clark, R. J. H., Hester, R. E., Eds.; Heyden: London, 1976; Vol. 2, Chapter 6.

(87) Lilley, T. H. In *Water—A Comprehensive Treatise*; Franks, F., Ed.; Plenum Press: New York, 1973; Vol. 3, Chapter 6.

ion that satisfies the requirement of forming a relatively stable hydrate in aqueous solution. The intrinsic nature of the potential here proposed is that of an effective one. Its simplicity joined to its first-principles quality guarantees a high performance in the time-averaged description of systems where many-body contributions are important. These potentials may facilitate the modeling of systems with a significant number of particles and long time simulations. Thus, salting effects and the counterion's role in the structure and dynamics of biomolecules,[15,16] charge, or mass transport in electrolyte or ionic strength effects on chemical reaction in solution are fair examples of those kinds of physicochemical phenomena where the potentials here described may be of great interest. In this line, the building of new potentials to describe the hydration of a set of other important cations is envisaged.

On the contrary, chemical phenomena that include important instantaneous electronic and nuclear changes, such as release of water molecules from the first hydration shell or ligand-exchange processes, cannot be described by the present scheme. We believe that two possibilities may be explored. The first is the combination of these potentials with AIMD or hybrid QM/MM methods such that the environment may be represented by the type of potentials here proposed whereas the zone of the solution where the processes take place is quantum mechanically described. In a second line of developments, we will seek to overcome the limitation imposed on water molecules to belong either to the first shell or to the bulk. This will open the door to investigate the mechanism of important reactions for many highly charged and transition metal cations in solution by means of MD simulations with reasonable computational effort, as has very recently been pointed out by Kowall et al.[89] in an ab initio study on the water-exchange reaction of Al^{3+}, Ga^{3+}, and In^{3+} in aqueous solutions.

Acknowledgment. We thank Spanish DGICYT for financial support (PB95-0549) and CICA (Centro Informatico Cientifico de Andalucia) for allocation of computer resources. We are grateful to reviewer A for his useful suggestions.

JA9830748

(88) Taube, H. *J. Phys. Chem.* **1954**, *58*, 523.
(89) Kowall, T.; Caravan, P.; Bourgeois, H.; Helm, L.; Rotzinger, F. P.; Merbach, A. E. *J. Am. Chem. Soc.* **1998**, *120*, 6569.